


Open Access Article

 <https://doi.org/10.55463/issn.1674-2974.50.6.6>

The Evaluation of the Drying Kinetics of Cassava Slices (*Manihot Esculenta* Crantz) Variety Ica Catumare

Rosemberg Alejandro Flórez Marín, Juan Carlos Lucas Aguirre*

Master in Agroindustrial Processes, Faculty of Agroindustrial Sciences, Universidad del Quindío, Armenia, Quindío, Colombia

* Corresponding author: jclucas@uniquindio.edu.co

Received: March 18, 2023 / Revised: April 10, 2023 / Accepted: May 9, 2023 / Published: June 30, 2023

Abstract: Convection drying of food and vegetables is a slow and energy-intensive process and takes a long time, up to 25 h, to complete the drying process depending on the drying conditions due to the high latent heat of vaporization of water, the low or limited rate of internal transport of water to the product surface, particularly in food, and the inefficiency of using hot air as drying medium. Accordingly, it is imperative to find the optimum drying conditions for economical operation. In this work, the effect of temperature (40, 50, 60, and 70°C) and the thickness of the slices (2, 4 and 6 mm) on the cassava drying process were evaluated. The samples of *Manihot Esculenta* Crantz, variety Ica Catumare (CM-523) were placed in perforated trays 12.5 cm * 13.1 cm with an air velocity of 2.34 m/s, leaving 70% free for drying air recirculation; drying time (t_s) and effective diffusivity (D_{eff}) and activation energy (E_a) of cassava slices were determined, conforming to mathematical models to describe drying kinetics. The results showed a significant effect of drying temperature and slice thickness, decreasing drying time as air temperature increases and slice thickness decreases, achieving a 93% reduction of the initial moisture in the cassava slices. The mathematical model that best described the kinetics behavior of the drying curves was Page with a linear regression ($0.995 \leq R^2 \leq 0.998$) and RMSE of 0.001–0.005. The effective diffusivity coefficient varied according to its thickness (2, 4, and 6 mm) between $3.164E^{-8}$ and $5.526E^{-8}$ m²/s, $1.568E^{-8}$ and $2.872E^{-8}$ m²/s, and $1.067E^{-8}$ and $1.967E^{-8}$ m²/s, respectively. The activation energy (E_a) varied between 19.092, 19.464, and 19.519 KJ/mol, which is within the ranges of agricultural products. Color changes of cassava slices were not negative considering the values of L^* , a^* and b^* ; achieving low values for a^* and b^* and high luminosity, usual characteristics of dry products. It was possible to determine the effect and influence of temperature on the reduction of cassava moisture content, observing an increase in the rate of free moisture loss with increasing temperature. The predominant period in drying was the decreasing period since most of the time is spent in this period.

Keywords: cassava, drying curves, mathematical modeling, color, diffusivity, activation energy.

伊卡·卡图马雷木薯片（木薯）干燥动力学评价

摘要：食品和蔬菜的对流干燥是一个缓慢且耗能的过程，需要很长时间（长达25小时）才能完成干燥过程，具体取决于干燥条件，因为水的汽化潜热较高，水的蒸发潜热较低或有限。水从内部输送到产品表面的速率，特别是食品中的水分，以及使用热空气作为干燥介质的低效率。因此，必须找到经济运行的最佳干燥条件。在这项工作中，评估了温度（40、50、60和70°C）和切片厚度（2、4和6毫米）对木薯干燥过程的影响。将木薯品种伊卡·卡图马雷（厘米-523）的样品置于12.5厘米*13.1厘米的多孔托盘中，空气流速为2.34 m/s，留

出70%的空间用于干燥空气再循环；确定了木薯片的干燥时间 (t_s)、有效扩散率 (德夫) 和活化能 (埃亚)，符合描述干燥动力学的数学模型。结果表明，干燥温度和切片厚度影响显著，随着气温升高和切片厚度减小，干燥时间减少，木薯切片初始水分减少了93%。最能描述干燥曲线动力学行为的数学模型是页，其线性回归 ($0.995 \leq R^2 \leq 0.998$) 和均方根误差为 0.001–0.005。有效扩散系数根据其厚度 (2、4和6毫米) 在 $3.164E-8$ 和 $5.526E-8$ 平方米/秒、 $1.568E-8$ 和 $2.872E-8$ 平方米/秒和 $1.067E-8$ 之间变化。和 $1.967E-8$ 平方米/秒分别。活化能(埃亚)在 19.092、19.464和19.519 千焦耳/摩尔之间变化，在农产品的范围内。考虑到 L^* 、 a^* 和 b^* 的值，木薯片的颜色变化不是负值；实现低 a^* 和 b^* 值以及高亮度，这是干燥产品的常见特征。通过观察自由水分损失率随温度升高而增加，可以确定温度对木薯水分含量降低的影响。干燥的主要时期是减少期，因为大部分时间都花在这个时期。

关键字： 木薯、干燥曲线、数学建模、颜色、扩散率、活化能。

1. Introduction

Cassava (*Manihot esculenta* Crantz), also known as 'tapioca', is a widely cultivated tuberous root shrub in most of sub-Saharan Africa, Latin America, Asia, and the Caribbean [1]-[2]. It is prized for its ability to thrive in adverse climate conditions [3]. Products such as cassava, because of its humidity between 60% and 65%, can have large postharvest losses due to the deficiency of technological mechanisms used in its conservation [4].

However, this food is difficult to preserve because it has two types of deterioration: primary and secondary. Primary deterioration, known as physiological deterioration, is a response to abiotic stress that appears 24 to 48 hours after harvest on the roots and manifests through physiological, biochemical, and ultrastructural changes [5]-[6]. This is characterized by brown coloration in the inner part of the root, which is generally the initial cause of the low acceptability of the product. Secondary deterioration, also called microbial, normally appears after physiological deterioration due to the action of a wide group of fungi and bacteria, mostly pathogens [7]. For this reason, modeling the drying curves of products of biological origin has become an alternative to understanding the phenomena that govern their behavior [8].

Convection drying is a unit operation, which consists in eliminating water with air through the simultaneous transfer of heat, mass, and momentum. The required heat is conducted on the food by a hot air current. Energy is transferred to the product surface through convection and then transferred within the product through diffusion or convection, depending on the structure of the product. Este heat flow causes increased temperature of the product and water evaporation. Humidity is transferred from the product surface to the air through convection as water vapor

and from within the product through diffusion, convection or capillarity. The drying speed and properties of the dry product depend on the external conditions of the process, such as air temperature, humidity, velocity, and direction of the air flow. In addition, the drying speed depends on the internal conditions like geometry, thickness, shape and structure of the product. The complexity of the structure and composition of the fruits, the variety of transport phenomena, and the biological variability make the drying of fruits a challenge [9]-[11].

The prediction of drying kinetics in raw materials under different conditions is very important to design processes and equipment, to supply sufficient energy and fuel, to select appropriate storage, to transfer materials, etc. At the same time, it allows sufficient tools for mathematical modeling and simulation, which are important to understand the complexity of drying, and also allows obtaining the right operating conditions through optimization [10]-[11].

The objective of this research was to determine the kinetics and kinetic parameters of drying cassava variety Ica Catumare to be used in the design of industrial cassava dryers due to the effect of air temperature and slice thickness, such as the effective diffusivity (D_{eff}) of water during drying and calculate the activation energy required to initiate humidity diffusion in the drying process.

2. Materials and Methods

To perform the research, cassava variety Ica Catumare (MC 523-6) was used with a vegetative period of 12 months; the raw material that was supplied by the marketer of agricultural products CORRELAG S.A, from the city of Armenia.

Initial moisture content on wet basis was determined by heating in an oven at 105°C for 24 h

until reaching constant weight [12] and was conducted in triplicate from three different lots and calculated using equation 1.

$$X(t) = \frac{M_t - M_s}{M_s} * 100\% \quad (1)$$

where M_t is the sample mass (g) on time, t , and M_s the mass of the totally dry sample (g).

2.1. Drying

The cassava slices were placed on perforated trays, then taken to a forced convection drying oven (APT.line™, Binder, Germany); which consists of a high-performance fan, powered by a 15 W motor, with two chrome grills, with a temperature range from 5 to 300 °C, the drying was carried out in triplicate at drying air temperatures of 40, 50, 60, and 70°C and air velocity of 2.34 m/s, humidity loss of the samples was determined throughout the drying period, weighing them every 5 min during the first 30 min, then every 15

min up to 2 h; thereafter, every 30 min until the samples reached constant weight, using an electronic digital scale (± 0.001 g) (Mettler Toledo and Columbus, USA).

2.2. Mathematical Determination of the Drying Kinetics Model

Five mathematical models were evaluated for the drying of foods and it was established which of these had a greater statistical fit in the drying of cassava. The models proposed were the Newton, Page, Henderson and Pabis, Wang and Sing and the logarithmic models (Table 1).

$$RMSE = \left[\frac{1}{N} \sum_{i=1}^N (MR_{mod} - MR_{exp})^2 \right]^{1/2} \quad (2)$$

To select the kinetic model, the coefficient of determination (R^2) and root mean square error were used as parameters ($RMSE$) (Equation 2).

Table 1 Mathematical models used in modeling the drying process (Compiled by the authors)

Mathematical modeling	Mathematical equation	Equations	Reference
Page model	$MR = \text{Exp}(-kt^n)$	Equation (3)	[13]
Henderson and Pabis model	$MR = a * \text{Exp}(-kt)$	Equation (4)	[14]
Wang and Singh model	$MR = 1 + at + bt^2$	Equation (5)	[15]
Newton's model	$MR = \text{Exp}(-kt)$	Equation (6)	[16]
Logarithmic model	$MR = a [\text{Exp}(-kt)] + C$	Equation (7)	[17]

Notes: MR is the moisture ratio, t is the drying time in hours, K is the drying constant (h^{-1}), a , b , c , n are the fit coefficients.

2.3. Determination of Effective Diffusivity and Activation Energy

The data derived from each work condition were replaced in Equation 2 and the moisture ratio (MR) of cassava was determined as a function of the drying time.

$$MR = \frac{X - X_e}{X_0 - X_e} = \frac{8}{\pi^2} \text{Exp} \left(\frac{-Df\pi^2 t}{4L^2} \right) \quad (3)$$

where X_t is the moisture in each of the study times, X_E is moisture in equilibrium, and X_0 is the initial moisture of cassava in $t = 0$, where: l = sample thickness (m), all moisture values are reported on dry base.

From the values derived from the mathematical model with the best statistical fit, the effective diffusivity coefficient (D_{eff}) was determined by applying Fick's second law (Equation 8). The effective diffusivity was obtained by plotting the MR logarithm in function of time (t), from which resulted a straight line from whose slope the D_{eff} was calculated for each temperature used. From the D_{eff} calculated, the Arrhenius equation (Equation 9) was used to determine the activation energy E_a (KJ/mol) in the cassava drying process for each operating condition used.

$$k_t = k_0 * e^{\frac{-E_a}{RT}} \quad (4)$$

with k_t being the speed of reaction, K_0 is the drying constant, E_a is the activation energy, R is the gas constant (8.314 J/mol °K), and T is the air temperature in °K, where plotting $\text{Ln}(D_{eff})$ vs. $(1/T)$ yields a straight line, whose slope is $(-E_a/R)$, which permits obtaining the activation energy [10], [13], [15]-[20].

2.4. Color Measurements

To determine the different color parameters in the samples analyzed, Minolta CM-2002R spectrophotometer was used. (Minolta Camera Co, Osaka, Japan) was calibrated with a standard green and white ceramic plate prior to reading. The three parameters in the model represent the color luminosity (L^*), $L^* = 0$ indicates black and $L^* = 100$ indicates white); their position between red and green (a^* , negative values indicate green, while positive values indicate red); and their position between yellow and blue (b^* , negative values indicate blue and positive values indicate yellow) [21].

2.5. Statistical Analysis

The data were analyzed statistically using a 4x3 factorial design (four drying temperatures, three slice thicknesses). Analysis of variance (ANOVA) and Tukey's test were applied to explain the effect of the drying temperatures and thickness ($p < 0.05$) on the loss of weight and the color parameters of the cassava slices during the drying process. This was performed using the Statgraphic® Plus Centurion.15.2.12 XV statistical package (Numagistics Ltd.).

3. Results and Discussion

3.1. Aspects of the Drying Process

Table 2 shows the factors that determined experimentally the drying process, evidencing that the results in terms of drying time and final moisture

reached according to the thickness of the cassava slices, which initially had humidity of $65.39 \pm 5.68\%$ for cassava, given that at the end of the drying process, cassava slices 2-mm thick had humidity of $3.027 \pm 0.43\%$, but increasing the thickness of the cassava

slices also increased the final moisture content of the samples under the same drying conditions for the cassava slices. It is noted that at a temperature of 40°C , the drying time and final moisture were higher than 50, 60, and 70°C .

Table 2 Drying times and final moisture at different thicknesses of cassava slices (Compiled by the authors)

Temperature ($^\circ\text{C}$)	Thickness (mm)	Final humidity (%)	Drying time (min)
40	2	3.960 ± 0.433	300
50		3.446 ± 0.437	240
60		3.056 ± 0.435	180
70		3.027 ± 0.430	135
40	4	4.786 ± 0.231	420
50		4.661 ± 0.239	360
60		4.412 ± 0.237	300
70		4.300 ± 0.235	270
40	6	5.576 ± 0.283	540
50		5.511 ± 0.286	480
60		5.274 ± 0.287	420
70		4.953 ± 0.289	360

When maintaining constant each of the drying temperatures ($40, 50, 60,$ and 70°C) with an air velocity of 2.34 m/s , it is noted that as the thickness of the cassava slices increases, the final humidity content increases, however, increasing the drying temperature diminishes the drying time in the cassava slices. As the circulating heat flow increases, the speed of heat and mass transfer increases with it, resulting in decreased drying time. Similar results were obtained in [22] with initial humidity of 57.0% for plantain and 64.5% for cassava, given that at the end of the process, the 0.20-cm thick raw material had a humidity of 6.80% for plantain and 6.84% for cassava. In turn as reported in [23], the initial moisture content of yam at $66.70 \pm 0.7\%$ (wet base).

3.2. Determination of Drying Kinetics

Figure 1 shows the behavior of the moisture content in dry base ($\text{Kg H}_2\text{O/Kg ss}$) with respect to the drying time (min) of the Ica Catumare (CM 523-7) cassava slices at different drying temperatures and slice thicknesses, and constant air velocity (2.34 m/s) in which it can be observed that moisture content reduces as drying time elapses. Overall, drying times reduce significantly with increased temperature of the drying air, with drying times being shorter with lower slice thickness.

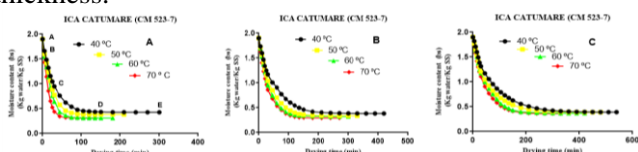


Fig. 1 Moisture content (bs) cassava slices with 2(A), 4(B), and 6(C)-mm thicknesses in the function of the drying time (Compiled by the authors)

This is how the times to reach each of the phases of the drying process A-B; B-C; CD; D-E are lower the higher the drying air temperature and the lower slice thickness, as the slopes of the curves are steeper in each

of the phases in all drying conditions.

Figure 1 shows the initial drying behavior of the cassava slices (A-B), the non-stationary phase was between 0 and 5 min, i.e, it takes a little while for cassava to reach equilibrium with the system. This is explained fundamentally by the internal physical structure of the particles of the cassava slices because they have lower porosity, therefore, the flow of internal water to the surface is slower.

With the moisture content constant period trend (B–C), as the process continues, the rate of moisture loss continues to decrease. In fact, the trend of the decreasing period of the moisture content (C–D) is due to the appearance of dry patches on the surface of the slices, causing water migration from its interior to the surface, which translates into the decrease of the slopes in this phase.

In Figures 1A, 1B, and 1C, the constant velocity period (B–C), which lasts between 15 and 25 min for all temperatures ($40, 50, 60,$ and 70°C) and all thicknesses (2, 4, and 6 mm) as the process continued, the rate of moisture loss continues decreasing between ($1.15 - 0.65 \text{ Kg H}_2\text{O/Kg SS}$) in ($1.24 - 0.96 \text{ Kg H}_2\text{O/Kg SS}$) and ($1.22 - 1.02 \text{ Kg H}_2\text{O/Kg SS}$); the second drying period at decreasing velocity lasts from 90 to 210 min, removing from the cassava slices a moisture content between ($0.47 - 0.31 \text{ Kg H}_2\text{O/Kg SS}$) in ($0.46 - 0.29 \text{ Kg H}_2\text{O/Kg SS}$) and ($0.45 - 0.31 \text{ Kg H}_2\text{O/Kg SS}$) until the solid reaches equilibrium.

Comparing times of different thicknesses and moisture loss during the drying period at a constant rate, cassava slices have different times for the three thicknesses. During the drying period at decreasing rate, it is observed that the time of duration and amount of moisture removed in the cassava slices diminish as drying time transpires, indicating that they have a final moisture content in the order of 3- 5%. Similar results were reported by [18] in the drying kinetics of plantain and cassava, obtaining a final moisture content in the

order of 7% to 8%; in [24] convection drying and elephant foot yam quality attributes; and in [22] in convection drying of cassava.

3.3. Determination of Drying Speed

Figure 2 shows the drying of cassava slices, evidencing the four phases that normally govern the drying of foods. The classic curves foods follow is presented [25], that is, there is a period of drying at a constant rate and a period of drying at a decreasing rate, the latter predominating during the process; therefore, it is the most studied in food drying. As the drying temperature increases, the moisture content decreases, but likewise, as the thickness of the cassava slices increases, the moisture content begins to lose less humidity. Hence, the predominant period in the drying of cassava slices is perceived (decreasing period) comprised of two phases (linear and asymptotic) which provide the highest percentage of free moisture (XL) reduction depending on the drying kinetics of the cassava slices; evidencing that for this first decreasing period the lower the temperature and the higher the thickness, the longer the drying time will be. In general terms, the rate of water elimination is higher when the temperature is increased, removing a high percentage of water. Subsequently, the period of asymptotic decreasing velocity begins in which moisture loss is much slower than that of the first period, indicating that water has great difficulty migrating to the surface due to the high retraction of the cassava slices caused by the great desiccation of the samples, which directly affects the reduction of the drying kinetics (R).

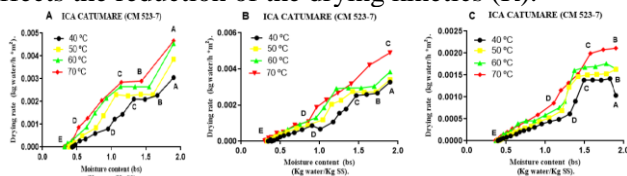


Fig. 2 Drying speed (R) cassava slices with 2(A), 4(B), and 6(C)-mm thicknesses in the function of the moisture ratio (XL) (Compiled by the authors)

Figures 2A, 2B, and 2C show an induction or

stabilization phase for an interval from 0 to 5 min in which the temperature of the samples increases over time, an initial loss of moisture content is evident (XL) (KgH₂O/Kg dry solid) from 32.6%–14.3% to 15.7%–9.7% and 12.5%–4.5%, but there is evidence of an increase in the maximum drying speed (R) achieved until the solid reaches equilibrium with the system. Likewise, the constant velocity period begins, which takes between 5 and 20 min in which a loss of moisture content (XL) (KgH₂O/Kg dry solid) of 25.8%–19.7% is evident in 23.7%–16.4% and 19%–14% when the drying speed (R) is reduced and remains constant; similarly, the period of decreasing velocity begins, comprising two phases. A first linear phase in which the decrease in moisture content (XL) is partially proportional to the decrease in drying speed (R), which evidences a loss of moisture content (XL) (KgH₂O/Kg dry solid) of 61.45%–39.22% in 47.5%–28.1% and 40.8%–24% in the drying kinetics of the cassava slices, a similar behavior was obtained in [18] in drying of plantain, in [26] and [27] in drying of pumpkin, and in [13] in drying of potato.

3.4. Mathematical Modeling of the Data Behavior in Cassava Drying Process

Table 3 shows the results where the R² values were > 0.98 for all mathematical models used except for the Wang and Singh model. Upon analyzing the data, it was observed that for three thicknesses the model that best fit the behavior of the data is the Page model with the highest R² values and lowest RMSE values but it is dependent on temperature. At the same time, the drying constant (k) obtained from the Page model serves to determine that the mathematical modeling of the process is a useful method to describe the relationship between the process parameters and the results of the convective drying of plantain and cassava [22]. Similar results were presented for drying yam [23]; likewise, these results agree with the other literature reported for drying cassava [18].

Table 3 Fit parameters of the drying kinetics of cassava slices for mathematical models (Compiled by the authors)

Methods	Parameters	Thickness 2 mm				Thickness 4 mm				Thickness 6 mm			
		40°C	50°C	60°C	70°C	40°C	50°C	60°C	70°C	40°C	50°C	60°C	70°C
Newton	R ²	0.9995	0.9966	0.9962	0.9964	0.9956	0.9993	0.9991	0.9982	0.9954	0.9960	0.9983	0.9986
	RMSE	0.000160	0.00509	0.00555	0.00576	0.00465	0.00199	0.00240	0.0033	0.00442	0.00425	0.00295	0.00276
	K	0.03427	0.04258	0.04894	0.07304	0.01986	0.02522	0.02946	0.03411	0.01347	0.01742	0.01991	0.02322
Wang and Singh	R ²	0.8322	0.9131	0.9061	0.8711	0.8719	0.9008	0.8915	0.8639	0.8902	0.8569	0.8884	0.9066
	RMSE	0.03209-0.01664	0.02580	0.02760	0.03448	0.02522	0.02456	0.05645	0.02919	0.02182	0.02565-0.00887	0.02424	0.02340
	a	0.000060	-0.0246	-0.0280	-0.0394	-0.01037	-0.01376	-0.01587	-0.01824	-0.00738	0.000017	-0.01048	-0.01320
Page	b	0.00013	0.00017	0.00033	0.000023	0.000042	0.000056	0.000075	0.000012	0.000024	0.000024	0.000024	0.000040
	R ²	0.9995	0.9985	0.9983	0.9988	0.9992	0.9993	0.9994	0.9994	0.9992	0.9996	0.9995	0.9995
	RMSE	0.00158	0.00331	0.00369	0.00329	0.00289	0.00199	0.00182	0.00189	0.00273	0.00244	0.00280	0.00169
Henderson and Pabis	k	0.03338	0.03001	0.03420	0.05109	0.02890	0.02523	0.02533	0.04298	0.02071	0.02583	0.02199	0.02837
	n	1.00783	1.11171	1.11825	1.13022	0.90435	0.99988	1.0436	0.93069	0.96023	0.90227	0.97453	0.94628
	R ²	0.9995	0.9968	0.9964	0.9967	0.9977	0.9993	0.9992	0.9985	0.9964	0.9968	0.9983	0.9983
Logarithmic	RMSE	0.00160	0.00488	0.00536	0.00552	0.00384	0.00199	0.00215	0.00296	0.00393	0.00386	0.00293	0.00250
	k	0.03431	0.04333	0.04978	0.07422	0.01891	0.02527	0.02996	0.03328	0.01294	0.01677	0.01978	0.02277
	a	1.00097	1.01596	1.01511	1.01620	0.96619	1.06566	1.01287	0.98212	0.97242	0.97404	0.99547	0.98624
Logarithmic	R ²	0.9967	0.9975	0.9971	0.9961	0.9970	0.9965	0.9993	0.9986	0.9965	0.9972	0.9983	0.9989
	RMSE	0.00151	0.00374	0.00479	0.00517	0.00383	0.00196	0.00207	0.00289	0.00386	0.00357	0.00293	0.00185
	k	0.03393	0.04169	0.04786	0.07214	0.01906	0.02507	0.02958	0.03379	0.01325	0.01743	0.01973	0.02319
Logarithmic	a	1.00333	1.02703	1.02676	1.02508	0.96478	1.00316	1.01558	0.97931	0.96785	0.96730	0.99661	0.98290
	c	-0.00390	-0.0159	-0.0160	-0.0114	-0.00245	-0.00277	-0.04504	-0.03379	-0.00738	-0.01210	-0.00092	-0.02319

Figure 3 shows the behavior of the drying constant, it presents an increase during the process as drying

temperature increases, however, with increased thickness of the cassava slices, a decrease in the values

of the k constant, for samples with 2-mm thickness at 40°C (0.03 min⁻¹), 50°C (0.04min⁻¹), 60°C (0.04 min⁻¹), 70°C (0.06 min⁻¹); 4-mm thickness at 40°C (0.01 min⁻¹), 50°C (0.02 min⁻¹), 60°C (0.03 min⁻¹), 70°C (0.04 min⁻¹); and for samples with 6-mm thickness, there is no significant change among the k values obtained at 40°C (0.01 min⁻¹), 50°C (0.01 min⁻¹), and 60°C (0.01 min⁻¹), unlike the value reached above 70°C (0.02 min⁻¹), which was the fastest. This behavior directly affects the behavior of drying speed as mentioned and shown in Figure 3.

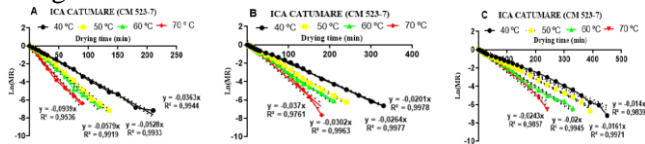


Fig. 3 Drying curve Ln (MR) Cassava slices with 2(A), 4(B), and 6(C)-mm thicknesses in the function of the drying time (Compiled by the authors)

In this study of both varieties, the D_{eff} for the conditions studied (Table 3) and the regression coefficients obtained were > 0.98, which were satisfactory results. The values obtained are within the range reported in the literature for various food products, 10⁻⁸ to 10⁻¹¹ m²/s, determining that said values can vary in the same species, depending on the slice thickness, conditions of the drying process, geometry and variety, as well as the thermo-physical properties of the product, and on the drying conditions, like temperature, relative humidity, and air-flow

velocity [10], [14], [17], [20], [28]-[29].

Table 4 shows the cassava effective diffusivity (D_{eff}) values, which increase as temperature increases at a constant air velocity; likewise, when slice thickness increases, the diffusivity coefficient decreases, bringing a considerable decrease in the internal resistance of food to free moisture migration. The decreased resistance provided by the food can be analyzed as the effect the rise in temperature exerts on the structure of the solid matrix, affecting the porosity of the cassava, which produces greater migration of water per surface area [10], [29].

This D_{eff} behavior is expected because it is a strong function of temperature that can be seen in the Arrhenius equation (Eq. 9). The higher the air temperature, the higher the surface temperature of the sample and therefore D_{eff} increase [26], [30]. Fick’s diffusion model assumes that diffusion occurs from only one direction, that is, from inside to the surface of the slices; this assumption is valid for thin slices in which lateral diffusion is insignificant [28].

Similar results are reported by Srikanth *et al*, (2019) [31] on convective drying of elephant foot yam (*Amorphophallus paeoniifolius*) for the D_{eff} , where diffusivity depends largely on the drying temperature and sample size, where increased drying air temperature increases the heat transfer and improves moisture movement and reduced sample size, yielding as a result greater moisture diffusivity.

Table 4 Effective diffusivity D_{eff} (m²/s) activation energy in the function of temperature and thickness of cassava slices (Compiled by the authors)

Temperature (°C)	Thickness (mm)	Diffusivity (m ² /s)	E_a (Kj/mol)	A (m ² /s)
40	2	3.164E10 ⁻⁸	19.092	3.881
50		3.538E10 ⁻⁸		
60		4.750E10 ⁻⁸		
70		5.526E10 ⁻⁸		
40	4	1.568E10 ⁻⁸	19.464	3.458
50		2.297E10 ⁻⁸		
60		2.808E10 ⁻⁸		
70		2.872E10 ⁻⁸		
40	6	1.066E10 ⁻⁸	19.519	3881
50		1.358E10 ⁻⁸		
60		1.741E10 ⁻⁸		
70		1.966E10 ⁻⁸		

The diffusivity coefficient indicates the speed with which water moves within the porous medium (cassava slices) due to the concentration difference; to interpret the drying process in the presence of hot air, where heat transfer occurs by convection from the supplied air to the surface of the product and by conduction from the contact surface of the sample container to the center of the product. The moisture loss or mass transfer that also includes volatile compounds in this type of stationary system is a diffusion mechanism according to Fick’s second law, which provides a connection between the effective moisture diffusivity and humidity ratio as well as the mass transport mechanisms [16], [17].

Such behavior occurs because at the beginning of the process there should be a rapid increase in temperature, which is the result of the difference between the temperature of the cassava slices and the air and the heat transferred by convection and the sensible heat for the temperature increase. When the surface of the slice reaches the air temperature, a moisture gradient is created between the surface and the inside of the slice, this gradient leads to moisture transport by diffusion from the inside of the product to the surface, where the physical nature of the fruit, the temperature, and its moisture content govern the internal diffusion and, consequently, the initial decrease in moisture [9]-[11].

At the air-surface interface, water evaporation occurs because the water concentration at the fruit surface exceeds the water concentration in the air, generating a water potential or a change in water concentration. This considers the moisture on the surface to be free water, causing “evaporative cooling” and could be considered the isosteric heat of sorption [14], [17].

After a while, the internal resistance controls the moisture transfer. Therefore, as the temperature of the fruit slowly rises toward air temperature, the moisture in the slice reaches a critical humidity and the drying process continues slowly due to the small gradients of moisture content. Finally, the process ends when the moisture vapor pressures inside the slice and that of the air reach equilibrium [19], [23]-[24].

The highest D_{eff} value observed in this study may be due to a higher drying temperature that improved activation energy, where activation energy is the energy required for humidity diffusion and indicates the sensitivity to temperature of the products. The value of the activation energy for humidity diffusion in most agricultural food products is between 12 and 110 kJ/mol, which corresponds to the values obtained in this study (Table 4). Similar results of activation energy values were found for different foods, like potato 20 KJ/mol [13]; yam from 17.5 to 21.49 KJ/mol [24]; cassava M-tai 33.66 to 16.16 KJ/mol [18], and mango

46.459 KJ/mol [32].

3.5. Color Measurements

The parameters of the CIELab coordinates, L^* , a^* , b^* , were measured to evaluate the effect of temperature and thickness of the cassava slices, finding that these did not show statistically significant differences ($p > 0.05$) except in the total color parameter (ΔE) with respect to the total color change of the dry samples with ($p < 0.05$) made up by the thickness difference of 2, 4, and 6 mm of the cassava slices.

Regarding color, overall drying provokes green darkening, evidenced by a decrease of the a^* values (negative) and a value with little color change difference in the b^* coordinate for cassava slices. The same behavior was seen in the L^* parameter with significance level $p > 0.05$. It is important to highlight that there is an increase in L^* values in dry cassava slices indicating surface whitening. The a^* parameter remains without important variations with central values in its position with respect to its green scale (negative values) and red, meaning an unimportant parameter in this type of product; it is evidenced that the b^* parameter with positive values (indicating yellow) is more important given that in cassava a white pigmentation associated with its composition is characteristic, although the appearance is predominantly yellow after drying.

Table 5 The color of dry cassava slices variety Ica Catumare at different temperatures and thicknesses (Compiled by the authors)

Temperature (°C)	Thickness (mm)	Coordinate (a)	P value	Coordinate (b)	P value	Luminosity (L)	P value	ΔE	P value
BLANCO	2	-1.067 ± 0.252	0.1998	16.167 ± 1.106	0.0000	70.333 ± 0.764	0.1333	0.00	0.0948
40		-0.918 ± 0.371		15.592 ± 1.314		72.015 ± 2.336		4.497 ± 1.660	
50		-1.059 ± 0.346		17.824 ± 1.404		72.267 ± 2.213		4.318 ± 0.783	
60		-1.083 ± 0.384		18.127 ± 1.398		72.528 ± 1.926		3.883 ± 1.535	
70		-1.108 ± 0.198		18.381 ± 0.931		73.901 ± 0.754		3.072 ± 1.415	
40	4	-0.775 ± 0.267	0.0750	15.755 ± 1.287	0.0000	71.963 ± 2.554	0.5199	3.478 ± 0.896	0.7714
50		-0.864 ± 0.308		16.729 ± 1.096		72.293 ± 1.211		3.293 ± 1.020	
60		-0.954 ± 0.240		17.639 ± 1.088		72.615 ± 2.084		3.257 ± 1.3	
70		-1.058 ± 0.334		18.355 ± 1.024		73.125 ± 0.948		3.006 ± 0.857	
40	6	-0.835 ± 0.24	0.2660	15.571 ± 2.251	0.0000	71.906 ± 2.022	0.1258	4.096 ± 0.917	0.0630
50		-0.875 ± 0.238		16.308 ± 0.956		72.125 ± 1.666		3.629 ± 1.196	
60		0.927 ± 0.345		17.567 ± 1.594		72.968 ± 2.422		3.155 ± 0.979	
70		0.109 ± 0.266		18.508 ± 1.291		73.423 ± 1.428		2.765 ± 0.922	

Table 5 displays the ΔE variation with change in temperature and thickness evaluated during the drying of the slices. It is evidenced that at a lower thickness, the total color change is higher, given that the material is exposed to direct heat from convective drying, but there is no evident enzymatic browning, the data reveal that as the temperature increases the color change (ΔE), although it presents differences statistically are not significant, the CIELab coordinates for products the $\Delta E= 1$, gives to understand that the color is the same, $\Delta E= 3$, there was a change in the samples as it can (see table 4) and $\Delta E= 5$, where the color change of the sample is considered not act, because it is provided a browning of this in the drying of food.

4. Conclusions

The knowledge of the speed of each stage will be

decisive to make decisions on process control in order to find a balance between the optimization of drying process (less time and energy expenditure) and the sensory and nutritional characteristics desired.

The air-drying temperature had much influence on the drying time, evidencing lower times with each increase in the drying temperature; similarly, lesser thickness of the cassava slices permitted obtaining lower drying time; Ica Catumare had drying times with 5% statistically significant level.

The drying curves permitted clearly identifying non-stationary period (A-B), constant period velocity (B-C) and decreasing period (C-D) at different temperatures and thicknesses studied.

The effective diffusivity (D_{eff}) of the cassava slices increased with increased temperature and diminished with increased thickness of the slices, but – in general –

it remained within a range of ($3.164E^{-8}$ to $5.526E^{-8}$ m^2/s); ($1.568E^{-8}$ to $2.872E^{-8}$ m^2/s) and ($1.067E^{-8}$ to $1.967E^{-8}$ m^2/s), and the activation energy (E_a) increases as the thickness increases in the study conditions worked, being higher, when the thickness was 6 mm (19.519 KJ/mol) and lower when the thickness was 2 mm (19.092 KJ/mol).

The mathematical model with the highest fit to the drying curves was Page model with a correlation coefficient between ($0.995 \leq R^2 \leq 0.999$) and MRSE ($0.001 \leq MAE \leq 0.005$). However, the Newton, exponential, Henderson, and Pabis-modified models had good mathematical fit to the drying curves.

D_{eff} is the key variable to describe the diffusion of moisture through food products during drying and at the same time these drying models allow not only to predict the best process but also offer tools to predict storage and packaging conditions, and help to establish the final moisture content of agricultural products and the requirements of the drying process.

Overall color changes did not have a very relevant effect on the drying kinetics of the cassava slices, but likewise the composition of the cassava slices has a white color, which influences the b^* coordinate that cassava slices turned from white to yellow and with a surface luminosity toward the whiter color.

References

[1] ABASS A B, AWOYALE W, ALENKHE B, et al. Can food technology innovation change the status of a food security crop? A review of cassava transformation into "bread" in Africa. *Food Reviews International*, 2018, 34(1): 87-102. <https://doi.org/10.1080/87559129.2016.1239207>.

[2] ARISTIZÁBAL J, GARCÍA J A, & OSPINA B. Refined cassava flour in bread making: a review. *Ingeniería e Investigación*, 2017, 37(1): 25-33. <https://dx.doi.org/10.15446/ing.investig.v37n1.57306>.

[3] EL-SHARKAWY M A. Global warming: Causes and impacts on agroecosystems productivity and food security with emphasis on cassava comparative advantage in the tropics/subtropics. *Photosynthetica*, 2014, 52(2): 161-178. <https://doi.org/10.1007/s11099-014-0028-7>.

[4] FALADE K O, OLURIN T O, IKE E, & AWORH O. Effect of pretreatment and temperature on air-drying of *Discorea alata* and *Discorea rotundata* slices. *Journal of Food Engineering*, 2007, 80(4): 1002-1010. <https://doi.org/10.1016/j.jfoodeng.2006.06.034>.

[5] BARRAGÁN-ALTURO M I, LÓPEZ J M, CADAVID L F, & LUCAS-AGUIRRE J C. *Manual de Tecnologías en la Cadena Agroindustrial de la Yuca (Manihot esculenta Crantz)*. Programa Nacional de Competitividad y Desarrollo Tecnológico en la Cadena Agroindustrial de Frutas y Hortalizas, SENA Dirección General, Dirección de Formación Profesional Grupo de Competitividad. Bogotá, Colombia. Impresora. Feriva S.A., 2002.

[6] WHEATLEY C C. Studies on cassava (*Manihot esculenta Crantz*) root post-harvest physiological deterioration. Ph.D. Thesis. University of London, UK, 1982.

[7] BOOTH R H. *Almacenamiento de raíces de yuca*. Causas del deterioro que se presenta después de la cosecha de raíces frescas. Centro Internacional de Agricultura Tropical. Cali,

Colombia, 1976.

[8] BRENNAN J C, BUTTERS J R, COWRELL R L, & LILLY A E. *Las Operaciones de la Ingeniería de los alimentos*. España: Editorial Acribia, 1980.

[9] CASTRO A M, MAYORGA E Y, & MORENO F L. Mathematical modelling of convective drying of fruits: A review. *Journal of Food Engineering*, 2018, 223: 152-167. <https://doi.org/10.1016/j.jfoodeng.2017.12.012>.

[10] DEFRAEYE T, & RADU A. Insights in convective drying of fruit by coupled modeling of fruit drying, deformation, quality evolution and convective exchange with the airflow. *Applied Thermal Engineering*, 2018, 129: 1026-1038. <https://doi.org/10.1016/j.applthermaleng.2017.10.082>.

[11] PURLIS E. Modelling convective drying of foods: A multiphase porous media model considering heat of sorption. *Journal of Food Engineering*, 2019, 263: 132-146. <https://doi.org/10.1016/j.jfoodeng.2019.05.028>.

[12] A.O.A.C. International. Official methods of analysis of AOAC International. 20 ed. Rockville (USA): AOAC International, 2006.

[13] SINGH P, & TALUKDAR P. Diseño y evaluación del rendimiento de un secador convectivo y predicción de las características de secado de la papa en condiciones variables. *Revista Internacional de Ciencias Térmicas*, 2019, 142: 176-187.

[14] ROMAN M C, FABANI M P, LUNA L C, et al. Convective drying of yellow discarded onion (Angaco INTA): Modelling of moisture loss kinetics and effect on phenolic compounds. *Information Processing in Agricultura*, 2020, 7(2): 333-341.

[15] RAMÍREZ-ESTRADA N, LÓPEZ-GONZÁLEZ C, GARCÍA-SUÁREZ F L, et al. Secado en Lote de Plátano Macho Verde (*Musa paradisiaca* L.) a Tres Temperaturas. IX Congreso de ciencia de los alimentos y V foro de ciencia y tecnología de alimentos, 2011, pp. 601-608.

[16] KOUKOUCH A, IDLIMAM A, ASBIK M, et al. Experimental determination of the effective moisture diffusivity and activation energy during convective solar drying of olive pomace waste. *Renewable Energy*, 2017, 101: 565-574. <https://doi.org/10.1016/j.renene.2016.09.006>.

[17] KAVEH M, SHARABIANI V R, CHAYJAN R A, et al. ANFIS and ANNs model for prediction of moisture diffusivity and specific energy consumption potato, garlic and cantaloupe drying under convective hot air dryer. *Information Processing in Agriculture*, 2018, 5: 372-387. <https://doi.org/10.1016/j.inpa.2018.05.003>.

[18] SALCEDO-MENDOZA J, MERCADO J L, VANEGAS M, et al. Cinética de secado de la yuca (*Manihot esculenta Crantz*) variedad CORPOICA M-tai en función de la temperatura y de la velocidad de aire. *Revista ION*, 2014, 27(2): 29-42.

[19] ROMAN M C, FABANI M P, LUNA L C, et al. Convective drying of yellow discarded onion (Angaco INTA): Modelling of moisture loss kinetics and effect on phenolic compounds. *Information Processing in Agricultura*, 2020, 7(2): 333-341.

[20] NADERY-DEHSHEIKH F, & TAGHIAN-DINANI S. Coating pretreatment of banana slices using carboxymethyl cellulose in an ultrasonic system before convective drying. *Ultrasonics – Sonochemistry*, 2019, 52: 401-413. <https://doi.org/10.1016/j.ultsonch.2018.12.018>.

[21] GARCÍA-MOGOLLÓN C, ALVIS-BERMÚDEZ A, & ROMERO-BARRAGÁN P. Capacidad de Rehidratación y Cambio de Color de Yuca (*Manihot esculenta Crantz*)

Deshidratada en Microondas. *Información Tecnológica*, 2016, 27: 53-60.

[22] CARRANZA J, & SÁNCHEZ M. Cinética de secado de Musa Paradisiaca L. plátano, y Manihot esculenta Grantz, yuca. *Revista amazónica de investigación alimentaria*, 2002, 2(1): 15-25.

[23] OJEDIRAN JO, OKONKWO CE, ADEYI AJ, et al. Características de secado de rodajas de ñame (*Dioscorea rotundata*) en un secador de aire caliente convectivo: aplicación de ANFIS en la predicción de la cinética de secado. *Heliyon*, 2020, 6(3), e03555.

[24] SRIKANTH K S, SHARANAGAT V S, KUMAR Y, et al. Secado por convección y atributos de calidad del ñame pata de elefante (*Amorphophallus paeoniifolius*). *LWT - Food Science and Technology*, 2019, 99: 8-16.

[25] GEANKOPLIS C. *Procesos de transporte y operaciones unitarias*. 2ª Edición, Editora Continental, México D.F, México, 1995.

[26] AGRAWAL S G, & METHEKAR R N. Mathematical model for heat and mass transfer during convective drying of pumpkin. *Food and Bioproducts Processing*, 2017, 101: 68-73. <https://doi.org/10.1016/j.fbp.2016.10.005>.

[27] ROJAS M L, & AUGUSTO P E D. Microstructure elements affect the mass transfer in foods: The case of convective drying and rehydration of pumpkin. *LWT - Food Science and Technology*, 2018, 93: 102-108. <https://doi.org/10.1016/j.lwt.2018.03.031>.

[28] KASHANINEJAD M, & TABIL L G. Drying characteristics of purslane (*Portulaca oleraceae* L.). *Drying Technology*, 2004, 22(9): 2183-2200. <https://doi.org/10.1081/DRT-200034268>.

[29] DAS I, & ARORA A. Alternate microwave and convective hot air application for rapid mushroom drying. *Journal of Food Engineering*, 2018, 223: 208-219. <https://doi.org/10.1016/j.jfoodeng.2017.10.018>.

[30] ZHAO P, GE S, MA D, et al. Effect of hydrothermal pretreatment on convective drying characteristics of paper sludge. *ACS Sustainable Chemistry & Engineering*, 2014, 2: 665-671.

<https://doi.org/10.1021/sc4003505>.

[31] SRIKANTH K S, SHARANAGAT V S, KUMAR Y, et al. Convective drying and quality attributes of elephant foot yam (*Amorphophallus paeoniifolius*). *LWT - Food Science and Technology*, 2019, 99: 8-16. <https://doi.org/10.1016/j.lwt.2018.09.049>.

[32] OCAMPO, A. Modelo cinético del secado de la pulpa de mango. *Revista EIA*, 2006, 3(5): 119-128.

参考文献:

[1] ABASS A B, AWOYALE W, ALENKHE B 等。食品技术创新能否改变粮食安全作物的现状？非洲木薯转化为“面包”的回顾。国际食品评论，2018，34(1): 87-102. <https://doi.org/10.1080/87559129.2016.1239207>。

[2] ARISTIZÁBAL J, GARCÍA J A 和 OSPINA B. 面包制作中的精制木薯粉：评论。工程与研究，2017，37(1): 25-33. <https://dx.doi.org/10.15446/ing.investig.v37n1.57306>。

[3] EL-SHARKAWY M A. 全球变暖：对农业生态系统生产力和粮食安全的原因和影响，重点是热带/亚热带木薯的比较优势。光合作用，2014，52(2): 161-178. <https://doi.org/10.1007/s11099-014-0028-7>。

[4] FALADE K O, OLURIN TO, IKE E, & AWORH O. 预处理和温度对盾叶薯蓣和薯蓣切片风干的影响。食品工程，2007，80(4): 1002-1010. <https://doi.org/10.1016/j.jfoodeng.2006.06.034>。

[5] BARRAGÁN-ALTURO M I、LÓPEZ J M、CADAVID L F 和 LUCAS-AGUIRRE J C. 木薯农工链技术手册（木薯）。水果和蔬菜农工链国家竞争力和技术发展计划，塞纳总局，专业培训局竞争力小组。哥伦比亚波哥大。打印机。费里瓦公司，2002年。

[6] WHEATLEY C C. 木薯(木薯)根收获后生理恶化的研究。博士论文。英国伦敦大学，1982

[7] BOOTH R H. 尤卡根的储存。造成图像损坏的原因。国际热带农业中心。哥伦比亚卡利，1976。

[8] BRENNAN J C、BUTTERS J R、COWRELL R L 和 LILLY A E. 食品工程操作。西班牙：社论阿克里比亚，1980。

[9] CASTRO A M、MAYORGA E Y 和 MORENO F L. 水果对流干燥的数学模型：综述。食品工程，2018，223: 152-167. <https://doi.org/10.1016/j.jfoodeng.2017.12.012>。

[10] DEFRAEYE T 和 RADU A. 通过对水果干燥、变形、质量演变以及与气流的对流交换进行耦合建模，深入了解水果对流干燥。应用热工，2018，129: 1026-1038. <https://doi.org/10.1016/j.appl Thermaleng.2017.10.082>。

[11] PURLIS E. 食品对流干燥建模：考虑吸附热的多相多孔介质模型。食品工程，2019，263: 132-146. <https://doi.org/10.1016/j.jfoodeng.2019.05.028>。

[12] A.O.A.C. 国际的。AOAC 国际的官方分析方法。第20版 罗克维尔(美国)：AOAC 国际，2006。

[13] SINGH P, 和 TALUKDAR P. 对流安全的预测和评估以及条件变量的安全性能的预测。国际科学杂志，2019，142: 176-187。

[14] ROMAN MC, FABANI M P, LUNA L C, 等。黄色废弃洋葱的对流干燥(安加科·国际商标协会)：水分损失动力学建模和对酚类化合物的影响。农业信息处理，2020，7(2): 333-341。

[15] RAMÍREZ-ESTRADA N、LÓPEZ-GONZÁLEZ C、GARCÍA-SUÁREZ F L 等。在三个温度下批量干燥猛男维德·普拉塔塔(芭蕉)。IX 食品科学与技术大会，2011，第 601-608 页。

[16] KOUKOUCH A, IDLIMAM A, ASBIK M 等。橄榄果渣废物对流太阳能干燥过程中有效水分扩散率和活化能的实验测定。可再生能源，2017，101: 565-574. <https://doi.org/10.1016/j.renene.2016.09.006>

[17] KAVEH M, SHARABIANI V R, CHAYJAN R A 等。用于预测对流热风干燥机下马铃薯、大蒜和哈密瓜干燥水分扩散率和单位能耗的 ANFIS 和神经网络模型。农业信息处理，2018，5: 372-387. <https://doi.org/10.1016/j.inpa.2018.05.003>。

[18] SALCEDO-MENDOZA J、MERCADO J L、VANEGAS M 等。尤卡电影(木薯)具有温度和空气速度功能的科波伊卡米泰变化。离子杂志，2014，27(2): 29-42。

[19] ROMAN MC, FABANI M P, LUNA L C, 等。黄色废弃洋葱的对流干燥(安加科·国际商标协会)：水分损失动力学建模和对酚类化合物的影响。农业信息处理，2020，7(2): 333-341。

- [20] NADERY-DEHSHEIKH F 和 TAGHIAN-DINANI S. 在对流干燥之前在超声波系统中使用羧甲基纤维素对香蕉片进行涂层预处理。超声波-声化学, 2019, 52: 401-413。 <https://doi.org/10.1016/j.ultsonch.2018.12.018>。
- [21] GARCÍA-MOGOLLÓN C、ALVIS-BERMÚDEZ A 和 ROMERO-BARRAGÁN P. 微波脱水丝兰(木薯)的补水能力和颜色变化。技术信息, 2016, 27: 53-60。
- [22] CARRANZA J, 和 SÁNCHEZ M. 芭蕉和木薯格兰茨, 尤卡的干燥动力学。亚马逊食品研究杂志, 2002, 2(1) : 15-25。
- [23] OJEDIRAN JO、OKONKWO CE、ADEYI AJ 等。热对流空气干燥机中辣根(薯蓣)干燥的特性: ANFIS 在干燥动力学预测中的应用。日光, 2020, 6(3), e03555。
- [24] SRIKANTH K S、SHARANAGAT V S、KUMAR Y 等。通过对流干燥和质量属性象脚(芍药魔芋)得名。轻重量-食品科学与技术, 2019, 99: 8-16。
- [25] GEANKOPLIS C. 运输过程和单元操作。第二版, 大陆出版社, 墨西哥 D.F, 墨西哥, 1995。
- [26] AGRAWAL S G, 和 METHEKAR R N.南瓜对流干燥过程中传热传质的数学模型。食品和生物产品加工, 2017, 101 : 68-73 。 <https://doi.org/10.1016/j.fbp.2016.10.005>。
- [27] ROJAS M L, 和 AUGUSTO P E D. 微观结构元素影响食品中的传质: 南瓜对流干燥和再水合的情况。轻重-食品科学与技术, 2018, 93 : 102-108 。 <https://doi.org/10.1016/j.lwt.2018.03.031>。
- [28] KASHANINEJAD M, 和 TABIL L G. 马齿苋(马齿苋)的干燥特性。干燥技术, 2004, 22(9): 2183-2200。 <https://doi.org/10.1081/DRT-200034268>。
- [29] DAS I, 和 ARORA A. 交替使用微波和对流热空气来快速干燥蘑菇。食品工程, 2018, 223 : 208-219。 <https://doi.org/10.1016/j.jfoodeng.2017.10.018>。
- [30] ZHAO P, GE S, MA D, 等。水热预处理对造纸污泥对流干燥特性的影响 ACS 可持续化学与工程, 2014, 2 : 665-671。 <https://doi.org/10.1021/sc4003505>。
- [31] SRIKANTH K S、SHARANAGAT V S、KUMAR Y 等。象脚山药(芍药魔芋)的对流干燥和质量属性。轻重量 - 食品科学与技术, 2019, 99 : 8-16 。 <https://doi.org/10.1016/j.lwt.2018.09.049>。
- [32] OCAMPO, A. 干燥芒果果肉的干燥动力学模型。环境影响评估杂志, 2006, 3(5): 119-128。